

RESEARCH

Open Access



# Somatostatin-expressing interneurons of prefrontal cortex modulate social deficits in the *Magel2* mouse model of autism

Xiaona Wang<sup>1\*</sup>, Mengyuan Chen<sup>1</sup>, Daoqi Mei<sup>2</sup>, Shengli Shi<sup>3</sup>, Jisheng Guo<sup>4</sup>, Chao Gao<sup>5</sup>, Qi Wang<sup>6</sup>, Shuai Zhao<sup>1</sup>, Xingxue Yan<sup>1</sup>, Huichun Zhang<sup>5</sup>, Yanli Wang<sup>5</sup>, Bin Guo<sup>7\*</sup> and Yaodong Zhang<sup>1\*</sup>

## Abstract

Dysfunction in social interactions is a core symptom of autism spectrum disorder (ASD). Nevertheless, the neural mechanisms underlying social deficits in ASD are poorly understood. By integrating electrophysiological, in vivo fiber photometry, viral-mediated tracing, optogenetic and pharmacological stimulation, we show reduced intrinsic excitability and hypoactivity of SOM interneurons in medial prefrontal cortex (mPFC) in *Magel2*-deficient mice, an established ASD model, were required to social defects. Chemogenetic inhibition of mPFC SOM-containing interneurons resulted in reduced social interaction in wild-type *Magel2* mice. These sociability deficits can be rescued by optogenetic activation by excitability of SOM in the mPFC and mPFC<sup>SOM</sup>-LS inhibitory pathway in *Magel2* knockout mice. These results demonstrate the hypoactivity for SOM action in the mPFC in social impairments, and suggest targeting this mechanism that may prove therapeutically beneficial for mitigating social behavioral disturbances observed in ASD.

**Keywords** Social deficits, Somatostatin, *Magel2*, Autism spectrum disorder, Medial prefrontal cortex

## Introduction

Autism spectrum disorder (ASD) refers to an early onset neurodevelopmental syndrome linked to deficits in impaired or abnormal social interactions [1]. Although many non-genetic factors have been associated with ASD, cumulative research has established a strong

causative relationship with genetics [2]. *Magel2* is a gene that is implicated in Prader-Willi (PWS) and Schaaf-Yang (SYS) syndromes and is categorized as one of the highest correlated gene to ASD risk, about 75–80% of SYS individuals meet formally the clinical diagnostic criteria of ASD [3]. Both of these genetic neurodevelopmental

\*Correspondence:

Xiaona Wang  
xiaonawang2015@163.com  
Bin Guo  
guobin@nxmu.edu.cn  
Yaodong Zhang  
syek@163.com

<sup>1</sup>Children's Hospital Affiliated to Zhengzhou University, Henan Children's Hospital, Zhengzhou Children's Hospital, Henan Key Laboratory of Children's Genetics and Metabolic Diseases, Henan Children's Neurodevelopment Engineering Research Center, Zhengzhou, China

<sup>2</sup>Department of Neurology, Children's Hospital of Suzhou University, Suzhou, China

<sup>3</sup>Department of Image, Children's Hospital Affiliated to Zhengzhou University, Zhengzhou, China

<sup>4</sup>Department of Pathology, School of Basic Medical Sciences, Yantai Campus of Binzhou Medical University, Yantai City, Shandong, China

<sup>5</sup>Department of Rehabilitation, Children's Hospital Affiliated to Zhengzhou University, Zhengzhou, China

<sup>6</sup>Department of Histology and Embryology, Guizhou Medical University, Guizhou, China

<sup>7</sup>School of Traditional Chinese Medicine, Ningxia Medical University, Yinchuan, Ningxia, China



© The Author(s) 2025. **Open Access** This article is licensed under a Creative Commons Attribution-NonCommercial-NoDerivatives 4.0 International License, which permits any non-commercial use, sharing, distribution and reproduction in any medium or format, as long as you give appropriate credit to the original author(s) and the source, provide a link to the Creative Commons licence, and indicate if you modified the licensed material. You do not have permission under this licence to share adapted material derived from this article or parts of it. The images or other third party material in this article are included in the article's Creative Commons licence, unless indicated otherwise in a credit line to the material. If material is not included in the article's Creative Commons licence and your intended use is not permitted by statutory regulation or exceeds the permitted use, you will need to obtain permission directly from the copyright holder. To view a copy of this licence, visit <http://creativecommons.org/licenses/by-nc-nd/4.0/>.

disorders have in common autistic symptoms with impairments in social behaviors that are persistent over the lifespan [4]. *Magel2*-deficient mice were shown to recapitulate pertinent phenotypes, manifesting altered social behaviors in adulthood [5, 6]. As such, understanding the neurobiological mechanisms that mediate social deficits is essential when exploring potential therapeutic strategies for treating ASD.

Both human and animal studies have implicated the medial prefrontal cortex (mPFC) as a critical brain area in the control of social interaction behaviors [7–11]. GABAergic (gamma-aminobutyric acidergic) interneurons play fundamental roles in social interaction and modulate cortical functions [12, 13]. Dysfunction of cortical interneurons leads to disruption of balanced excitation and inhibition and is closely linked to social dysfunction [14, 15]. It has been confirmed that cortical interneurons consist of multiple subgroups that display distinct molecular, electrophysiological and active properties [16, 17]. In particular, somatostatin (SOM)-containing interneurons comprise a subpopulation of approximately 30% of all cortical interneurons [18]. SOM interneurons preferentially target the dendrites of excitatory neurons, providing feedforward inhibition to the network activity [19]. It was unequivocally established that inhibition of SOM interneurons in the mPFC abolishes affective state discrimination in mice [20]. Also, SOM interneurons is involved in social withdrawal across cingulate cortex [21]. Although great progress has been achieved, knowledge with regards to the mechanisms modulating sociability of mPFC SOM interneurons in the *Magel2* mouse model of ASD is lacking.

The mPFC is well-known to be a hub that regulates social behaviors through its distinct output connections with the lateral septum (LS) [14], which is associated with the regulation of motivated behaviors including social interactions [22–24]. Recent efforts have demonstrated that lateral septum is crucial for regulating social novelty in mice [25]. The release of mPFC neuropeptide corticotropin-releasing hormone from to LS suppresses interaction with familiar mice [22]. Similarly, Bredewold et al., showed GABA neurotransmission in the LS modulates social play behavior in mice [26]. Furthermore, chemogenetic activation of LS GABA interneurons enhanced social behaviors [27]. Marta et al., reported that the mPFC projects to lateral septum to regulate food-rewarded learning [28]. The activation of the piriform cortex to lateral septum pathway during chronic social defeat stress is critical for the induction of behavioral disturbance [29]. It was assumed that SOM interneurons target different components of subcortical circuits to orchestrate anxiety and defensive response [30, 31]. Nevertheless, the precise functional roles of connections between mPFC and LS region, particularly

SOM-expressing GABAergic neuronal projections in *Magel2*-deficient mice, remain elusive regarding social impairments, necessitating further investigation.

In the current study, the homozygous transgenic mice for SOM-Cre and *Magel2* knockout (KO) exhibited social impairments similar to the ASD symptoms. By integrating electrophysiological, in vivo fiber photometry, viral-mediated tracing, optogenetic, and pharmacological stimulation, we proved that the decreased intrinsic excitability and hypoactivity of SOM interneurons in the mPFC played a vital role in social interaction deficits of *Magel2*-null animals. Also, we found that chemogenetic inhibition of SOM-expressing neurons induced social interaction impairments. Optogenetic manipulation of these neurons in the mPFC attenuated social deficits in *Magel2* KO mice. We further revealed a monosynaptic circuit from GABAergic projections from mPFC SOM-positive neurons to downstream LS mediated social impairments. Together, these results show that the mPFC<sup>SOM</sup>-LS pathway is critical for deficits in social behaviors in *Magel2*-deficient animals relate to ASD.

## Methods

### Animals

All the conducted experiments were approved by the Animal Care and Use Committee of Zhengzhou University. SOM-Cre/*Magel2* KO mice were generated by breeding SOM-Cre (Jackson Laboratory, Stock No: 013044) with *Magel2*<sup>tm1Stw/J</sup> mice (Jackson Laboratory, Stock No: 009062). Genotyping primers and protocols are as recommended by the manufacturer. Food and water were available ad libitum. All animals were housed in a stable environment (23–25 °C and 50% humidity). Mice were housed in a 12 h light/dark cycle (07:00–19:00 schedule). Experiments were run during the light phase (within 10:00–17:00). All the experiments were performed in male mice (8–10 weeks old). Every effort was made to minimize animal suffering.

### Three-chamber social interaction test

Sociability testing was performed using a three-chamber plexiglas box apparatus, as we have been previously described [32]. The test was carried out under low intensity conditions (5 lx). The three-chamber box (60×40×20 cm) contained dividing walls with 10 cm wide rectangular openings to enable free access of each chamber. The test mouse was placed in the central compartment and allowed free exploration of the test arena for a 10 min acclimation period. Afterwards, in a second phase (sociability), a novel mouse (sex and strain were matched with the subject mouse) was placed inside cage in the corner of each side chamber designated as the social chamber. The opposite chamber with an empty cage was designated as the neutral chamber. The test

mouse was allowed to freely explore new environment for another 10 min. The amount of time spent in each compartment, and time spent in sniffing or interacting with unfamiliar animal were recorded by the camera-assisted ANY-Maze software (Stoelting Co., IL, USA). The social preference index (discrimination index) was quantified by the following formula: (investigation time with an unfamiliar mouse - investigation time with empty cage)/investigation time with novel mouse + investigation time with empty cage) [33, 34].

### Open field

The open field test was carried out by placing the animal in the center of an open field area with opaque walls (50×50×50 cm) in a dimly lit (30 lx) room. Mice were allowed to freely explore for 30 min. The behavior of each animal was monitored via video recording. The total distance traveled and time spent in the center zone (25×25 cm) were calculated.

### Viral injections

Stereotaxic surgery was performed as we previously published protocol [32]. Mice were anesthetized with 1% isoflurane and placed in a stereotaxic frame (Xinglin Life Tech., Beijing, China) with a heating pad to maintain body temperature. A small craniotomy was made under a surgical microscope with a dental drill through which to inject the virus by a glass micropipette (tip diameter: 20 μm). A small volume of virus solution (200 nL; OBio Technology, China) at a rate of 50 nL/min was targeted into mPFC (AP: + 2.00 mm; ML: ± 0.30 mm; DV: -1.7 mm) or LS (AP: +0.5 mm; ML: ± 0.40 mm; DV: -3.0 mm) according to the Paxinos and Franklin mouse brain atlas (2nd edition). The injection pipette was left in place for another 10 min before the withdrawal. Experiments were performed 3 weeks after the virus injection.

For the fiber photometry experiments, we injected the unilateral mPFC of SOM-Cre/*Magel2* WT or SOM-Cre/*Magel2* KO mice with recombinant AAV2/9-hSyn-FLEX-jGCaMP7s-WPRE (titer:  $5.56 \times 10^{12}$  vg/mL).

For the chemogenetic inhibition of SOM interneurons in SOM-Cre/*Magel2* WT mice, we bilaterally injected the mPFC with AAV2/9-hSyn-DIO-hM4D(Gi)-mCherry-WPRE (titer:  $5.38 \times 10^{12}$  vg/mL), or AAV2/9-hSyn-DIO-mCherry-WPRE (titer:  $5.51 \times 10^{12}$  vg/mL).

For the experiments of selective optical activation of SOM interneurons, we bilaterally injected the mPFC with AAV2/9-hSyn-DIO-hChR2(H134R)-mCherry-WPRE (titer:  $5.30 \times 10^{12}$  vg/mL), AAV2/9-hSyn-DIO-mCherry-WPRE (titer:  $3.54 \times 10^{12}$  vg/mL) in SOM-Cre/*Magel2* KO mice.

For retrograde tracing of mPFC projections to the LS, we injected retro-AAV2- hSyn-DIO-mCherry-WPRE

(titer:  $6.75 \times 10^{12}$  vg/mL) into the bilateral LS of SOM-Cre/*Magel2* KO mice.

### Fiber photometry

A fiber photometry system (ThinkerTech, Nanjing, China) was used to record the calcium signals from the mPFC. Optic fiber with ceramic ferrule (diameter: 2.5 mm, ThinkerTech) was implanted in the ipsilateral mPFC (+AP: 2.00 mm; ML: +1.80 mm; DV: -1.50 mm) 3 weeks after GCaMP7s virus injection. The excitation light with the intensity of 40 μW was applied. Mice underwent fiber photometry recording were performed in a three-chamber social interaction test. Photometry data were imported to MATLABR2020b Mat files for further analysis. Calcium signal changes were described as the delta fluorescence/fluorescence ( $\Delta F/F_0$ ) as  $(F-F_0)/F_0$ , where  $F_0$  is the baseline fluorescence signal. Events were considered as the peak that exceeded the mean by 1 standard deviation. The area under the curve was identified as mean  $\Delta F/F$  of the event.

### Optogenetic manipulation

The optical fiber implantation was implemented 3 weeks ahead of behavioral testing. A 200-μm-diameter optical fiber (numerical aperture: 0.37; Inper Inc., Hangzhou China; ) was introduced into the targeting brain regions (with the tip 200 μm above) via the craniotomy. For optogenetic manipulation, the optical fiber was implanted to target unilateral mPFC or LS using the following coordinates: mPFC (AP: +2.00 mm; ML: ±1.80 mm; DV: -1.50 mm) and LS (AP: +0.5 mm; ML: ± 0.40 mm; DV: -2.8 mm). The ceramic ferrule was secured to the skull with 3 M Vetbond™ tissue adhesive and dental cement. In the three-chamber social test, blue light stimulation (wavelength, 470 nm; frequency, 20 Hz; width, 10 ms; power, 5–8 mW) was directed through the implanted optical cannula at the mPFC or LS during the light-ON stage. The control (mCherry) group underwent the same procedure and received the same amount of photostimuli.

### Immunofluorescence

As we previously described [32], mice were deeply anesthetized with isoflurane briefly and transcardially perfused with 4% paraformaldehyde (PFA). Brains were post-fixed in 4% PFA for overnight at 4 °C and equilibrated in 30% sucrose. Tissues were sectioned at 30 μm using a freezing vibratome (Leica Microsystems, Mannheim, Germany) in 0.1 M phosphate-buffered saline (PBS). The sections were exposed to the blocking solution that composed of 3% bovine serum albumin, 0.25% Triton X-100, and 3% goat serum in 0.1 M PBS. Subsequently, sections were incubated with rabbit anti-SOM antibody (1:1000; Peninsula Lab, San Carlos, CA;

Cat#HPA019472) overnight at 4 °C. The Alexa Fluor®488-conjugated donkey anti-rabbit IgG (1:600; Invitrogen, San Diego, CA, USA; Cat# R37118) was the secondary antibody. Sections were washed in PBS and mounted on gelatin-coated slides. Sections were then optically scanned with the Zeiss 980 laser scanning confocal microscope (Carl Zeiss AG, Jena, Germany). In accordance with previous studies [35], we quantified the soma in at least four sections near the center of the injection site, determined based on the immunofluorescence intensity of hM4D-mCherry-positive, ChR2-mCherry-positive, SOM-positive, or SOM-negative neurons.

### Slice electrophysiology

Whole-cell patch-clamp recordings were performed in acute brain slices from behaviorally modeled mice or those that had been stereotaxically injected with recombinant AAV-virus as we described previously [32, 36]. Mice were deeply anesthetized with isoflurane and perfused transcardially with ice-cold oxygenated (saturated with 95% O<sub>2</sub>/5% CO<sub>2</sub>) cutting solution containing the following: 120 choline chloride, 1.25 NaH<sub>2</sub>PO<sub>4</sub>, 26 NaHCO<sub>3</sub>, 2.5 KCl, 7 MgCl<sub>2</sub>, 0.5 CaCl<sub>2</sub>, 25 glucose, 5 sodium ascorbate and 3 sodium pyruvate (300–305 mOsm/L). After decapitation, the whole brain was rapidly dissected. Coronal brain slices (300 μm in thickness) containing the mPFC or LS were sectioned using a vibratome (5100 mZ, Campden Instruments, Loughborough, United Kingdom) in the cutting solution and then incubated in oxygenated artificial cerebrospinal fluid (ACSF) containing the following (in mM): 125 NaCl, 2.5 KCl, 10 glucose, 2 MgSO<sub>4</sub>, 2.5 CaCl<sub>2</sub>, 1.25 NaH<sub>2</sub>PO<sub>4</sub>, and 26 NaHCO<sub>3</sub> (pH 7.35); osmolarity, 290 to 300 mOsm/L. Slices were allowed to recover at 32 °C for at least 1 h before use. Then, the brain slice was transferred to a submerging recording chamber and continuously perfused with ACSF (2.5 ml/min, bubbled with 95% O<sub>2</sub>/5% CO<sub>2</sub>) at 32 °C by the temperature controller (Warner Instruments, Holliston, USA). Fluorescently-labeled cells were visualized with an upright microscope (Eclipse FN1, Nikon, Tokyo, Japan) equipped with differential interference contrast optics. Patch electrodes (5–7 MΩ) were pulled by P97 pipette puller (Sutter Instruments, Novato, CA, USA) from borosilicate glass (OD 1.5 mm, ID 0.86 mm). Data were sampled at 10 kHz and filtered at 2 kHz with the EPC 10 amplifier and PatchMaster v2.54 (HEKA, Lambrecht, Germany). If series resistance changed by >20% during recording, the data were discarded.

To assess the excitability of mPFC SOM interneurons under different experimental conditions, firing activities following current injections (1s duration and 0 to 300 pA intensity with 20 pA increment) were recorded with an internal solution containing the following: 130 potassium gluconate, 2 NaCl, 10 HEPES, 2 Mg-adenosine

5'-triphosphate, 0.3 Na<sub>3</sub>-guanosine 5'-triphosphate, 1 EGTA, and 8 NaCl (290–300 mOsm/L, pH 7.2 with KOH). The threshold current for firing (rheobase) was defined as the minimum current required to elicit at least one spike. Additional properties of action potentials were measured, including resting potential, half-width duration, afterhyperpolarization amplitude, and firing frequency of spike response.

To test the monosynaptic and inhibitory connection of the mPFC-LS, light-evoked inhibitory postsynaptic currents (eIPSCs) were recorded at -70 mV using electrodes filled with high chloride internal solution contained (in mmol/L): 145 CsCl, 2 Mg-ATP, 10 HEPES, 2 CaCl<sub>2</sub>, 5 QX-314 and 10 EGTA (pH 7.25–7.30, 294–297 mOsm/L). Tetrodotoxin (TTX, 1 μmol/L, Tocris Bioscience, Ellisville, MO, USA; Cat#1078), and 4-aminopyridine (4-AP, 100 μmol/L, Sigma; Cat#275875) were used to block multisynaptic connections. Picrotoxin (PTX, 50 μmol/L, Sigma; Cat#P1675) was added to block the GABA<sub>A</sub> receptor-mediated eIPSCs.

### In vivo multi-channel electrode recordings

Adult SOM-Cre mice were injected (200 μl/site) with recombinant rAAV vectors into the mPFC bilaterally as described above. Recordings were carried out at 3 weeks post-injection. The optrode was constructed with 16 single electrodes and an optic fiber (25 mm length). SOM-Cre/*Magel2* KO mice were implanted with optrodes targeting the mPFC at the same location where the virus was injected. Silver wires with three screws were attached to the skull as ground. Mice were habituated with the headstage and cables connected to the electrode on their heads for 7 days. Electrophysiological signals and social interaction data were simultaneously acquired using 16-channel Omniplex recording system (Plexon, Dallas, TX, United States). Spiking activities with amplitude larger than 3.5 standard deviations from the mean were digitized at 44 kHz, bandpass filtered from 300 Hz to 5000 Hz.

In blue light stimulation studies, animals received 20 Hz blue light stimulation in a 10 seconds on, 10 s off, pattern at 12 mW. Spikes with shorter half-spike width, half valley width and higher firing rate were considered as putative GABAergic interneurons [37].

For chemogenetic inhibition experiments, Clozapine-N-Oxide (CNO; Sigma, C0832) was dissolved in sterile saline (0.9% NaCl solution) to a concentration 0.5 mg/mL. CNO (5 mg/kg) was administered via an intraperitoneal injection to the hM4D transfected mice 30 min prior to behavioral testing based on an earlier report [38]. The control mice injected with mCherry under the same operating conditions was carried out.

### Statistical analysis

Data are presented as the mean  $\pm$  standard error of the mean (SEM). All statistical analysis and graphing were performed using Graphpad Prism 9.5 (GraphPad Software Inc.). All data were first checked for the normality and homogeneity of variance. The data were statistically analyzed using unpaired Student's *t*-test, one-way analysis of variance (ANOVA) followed by with Tukey's *post hoc* test. Statistical significance was set at  $p < 0.05$ .

## Results

### SOM-Cre/Magel2 KO mice exhibit impaired sociability

We first sought to target SOM interneurons in mice lacking *Magel2*, which required generation of new mouse lines. We bred SOM-Cre homozygous female mice with *Magel2* KO male mice. After several generations, SOM-Cre homozygous/*Magel2* homozygous KO and SOM-Cre/*Magel2* WT (WT) littermates were acquired accompanied with SOM-Cre homozygous/*Magel2* heterozygous mice, which were bred for subsequent generations (Fig. 1A). As illustrated in Fig. 1B-E, in the sociability test analyzing the total time spent in the three compartments, *Magel2* WT mice spent remarkably more time in the chamber of a novel mouse (NM) relative to the novel object (empty cage, NO) (NO =  $144.70 \pm 3.82$  s,  $n = 10$ ; NM =  $313.10 \pm 1.75$  s,  $n = 10$ ;  $p < 0.001$ ). However, no discernible difference in time spent in exploring two compartments was detected in SOM-Cre/*Magel2* KO (KO) animals (NO =  $246.40 \pm 3.50$  s,  $n = 10$ ; NM =  $250.30 \pm 5.47$  s,  $n = 10$ ;  $p = 0.56$ ). In the sociability test analyzing interaction time, *Magel2* WT mice exhibited more interactions with the novel mouse in comparison with the novel object (NO =  $59.10 \pm 2.14$  s,  $n = 10$ ; NM =  $152.40 \pm 5.14$  s,  $n = 10$ ;  $p < 0.001$ ). Nonetheless, *Magel2* KO mice spent similar time sniffing the novel mouse and the novel object (NO =  $113.10 \pm 2.88$  s,  $n = 10$ ; NM =  $117.40 \pm 2.59$  s,  $n = 10$ ;  $p = 0.28$ ). Furthermore, *Magel2* KO animals displayed a significantly lower discrimination index than that of the control group (WT =  $0.44 \pm 0.02$ ,  $n = 10$ ; KO =  $0.02 \pm 0.02$ ,  $n = 10$ ;  $p < 0.001$ ). In the open field test, no detectable differences in locomotor activity in 5 min intervals [at 5 min, WT =  $11.34 \pm 0.10$ ,  $n = 10$ ; KO =  $11.35 \pm 0.16$ ,  $n = 10$ ;  $p = 0.97$ ; at 10 min, WT =  $11.14 \pm 0.04$ ,  $n = 10$ ; KO =  $11.03 \pm 0.08$ ,  $n = 10$ ;  $p = 0.22$ ; at 15 min, WT =  $10.59 \pm 0.06$ ,  $n = 10$ ; KO =  $10.60 \pm 0.10$ ,  $n = 10$ ;  $p = 0.94$ ; at 20 min, WT =  $10.47 \pm 0.13$ ,  $n = 10$ ; KO =  $10.41 \pm 0.22$ ,  $n = 10$ ;  $p = 0.82$ ; at 25 min, WT =  $10.19 \pm 0.14$ ,  $n = 10$ ; KO =  $10.13 \pm 0.13$ ,  $n = 10$ ;  $p = 0.73$ ; at 30 min, WT =  $0.44 \pm 0.02$ ,  $n = 10$ ; KO =  $0.02 \pm 0.02$ ,  $n = 10$ ;  $p = 0.001$ ], total distance (WT =  $63.69 \pm 0.17$ ,  $n = 10$ ; KO =  $63.46 \pm 0.21$ ,  $n = 10$ ;  $p = 0.42$ ), and time spent in the center (a measure of anxiety-like behavior) (WT =  $65.18 \pm 0.35$ ,  $n = 10$ ;

KO =  $64.85 \pm 0.45$ ,  $n = 10$ ;  $p = 0.57$ ) of the open-field apparatus were found within these two groups (Fig. 1F-I). Overall, these data indicate social interaction deficits in SOM-Cre/*Magel2* KO mice.

### SOM interneurons in the mPFC are less excitable in *Magel2* KO mice

The mPFC is well recognized as the executive center of the brain, combining internal states and execute goal-directed behavior, including social actions [14]. To further explore SOM function in *Magel2* KO mice, we investigated the electrophysiological characteristics of mPFC SOM neurons using whole-cell patch-clamp recordings. We used SOM-Cre/*Magel2* WT and SOM-Cre/*Magel2* KO double-transgenic mice and stereotaxically injected AAV-DIO-ChR2-mCherry into the mPFC. After waiting 3 weeks for full expression of the virus, we recorded from SOM interneurons under the current-clamp model. Fluorescent mCherry, carried by the virus, enabled identification of SOM neurons under the microscope (Fig. 2A). Representative traces of action potential using 200 pA depolarizing current injection was shown in Fig. 2B. We examined the passive membrane property and intrinsic excitability of SOM interneurons in the current-clamp mode. No significant differences in the resting membrane potential (WT =  $-66.91 \pm 0.46$  mV,  $n = 14$  from 6 mice; KO =  $-67.64 \pm 0.54$  mV,  $n = 14$  from 6 mice;  $p = 0.32$ ) and half-width (WT =  $0.57 \pm 0.01$  ms,  $n = 14$  from 6 mice; KO =  $0.56 \pm 0.01$  ms,  $n = 14$  from 6 mice;  $p = 0.55$ ) of evoked action potential were observed between two groups (Fig. 2C-D). Nevertheless, the current threshold of SOM neurons was markedly increased in *Magel2* KO mice (WT =  $35.00 \pm 0.98$  pA,  $n = 15$  from 6 mice; KO =  $65.00 \pm 0.98$  pA,  $n = 15$  from 6 mice;  $p < 0.001$ , Fig. 2E). The mean amplitude of the afterhyperpolarization of SOM cells was reduced in *Magel2* KO animals (WT =  $21.18 \pm 0.22$  mV,  $n = 14$  from 6 mice; KO =  $18.00 \pm 0.15$  mV,  $n = 14$  from 6 mice;  $p < 0.001$ , Fig. 2F). Furthermore, we observed the drastic decreases in the action potential discharge frequency in response to depolarizing steps from 200 to 300 pA in slices from *Magel2* KO animals relative to that of SOM-Cre/*Magel2* WT mice (depolarizing steps ranging from 200 to 240 pA,  $p < 0.001$ ; 260 pA depolarizing steps,  $p = 0.0039$ ; 280 pA depolarizing step,  $p = 0.0001$ ; 300 pA depolarizing steps,  $p = 0.0012$ ;  $n = 12$  from 6 mice per group, Fig. 2H). However, the spike frequency was comparable during depolarizing steps from 80 to 180 pA in slices between two groups (all  $p > 0.05$ , Fig. 2G). The results of these experiments therefore showed that mPFC SOM interneurons are less excitable in *Magel2* KO mice and they may be responsible for the impairment in social interaction defects.

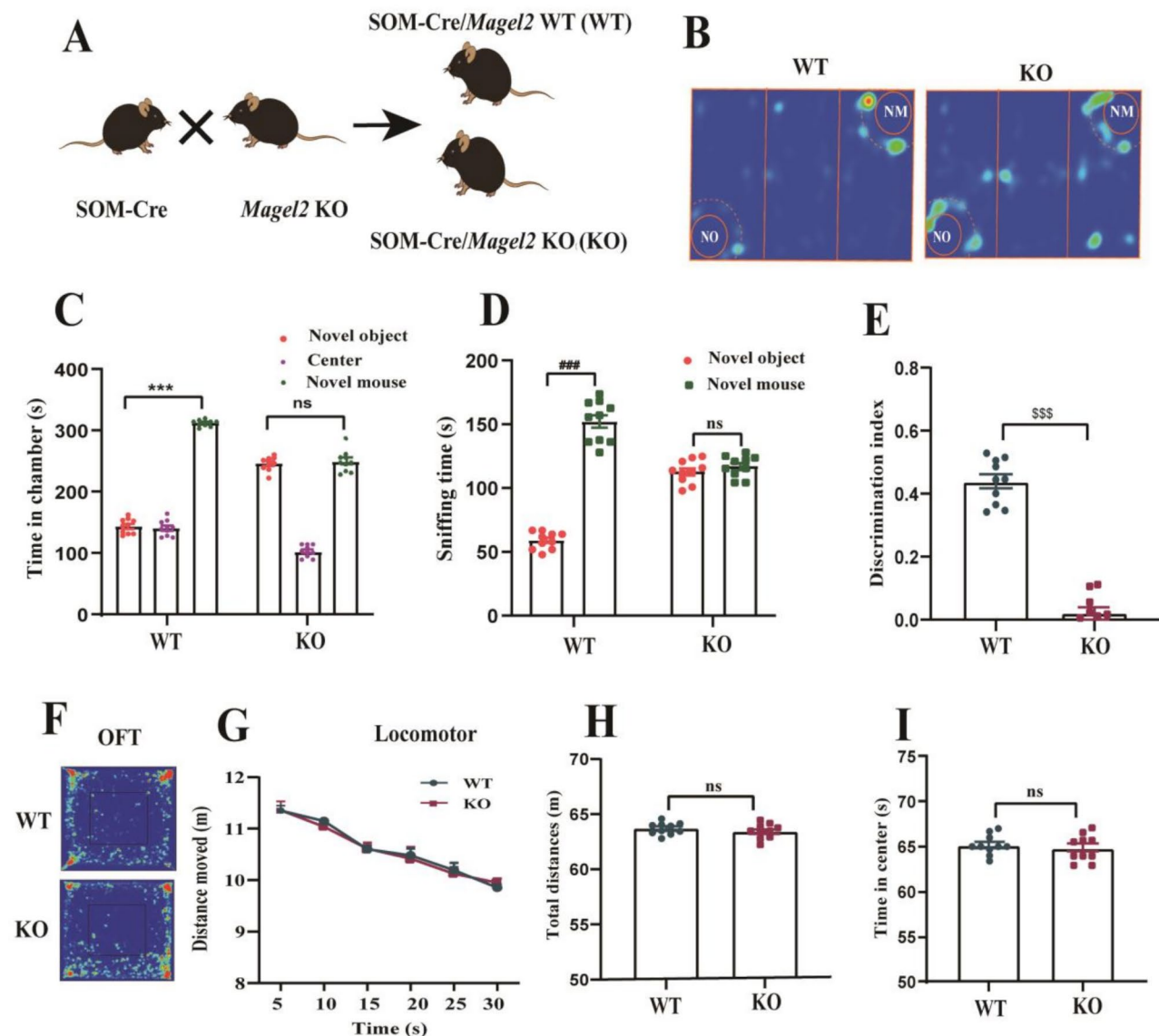


**Fig. 1** Impaired sociability of the SOM-Cre/*Magel2* KO mice. **A** Breeding strategy to generate SOM-Cre/*Magel2* KO (KO) mice is displayed. **B** Representative heat map from each group in the social interaction test. **C** During the sociability test, SOM-Cre/*Magel2* WT (WT) mice spent prominently more time in the chamber of the unfamiliar mouse in comparison to the novel object. No significant difference in the time spent exploring the chamber containing the novel mice relative to the familiar chamber for KO mice. **D** WT mice spent more time sniffing the novel mouse relative to empty cage (novel object). In contrast, KO mice spent equal amounts of time sniffing the novel mouse and the novel object. **E** WT mice had a significantly lower discrimination index than control mice. **F** Representative images displaying the exploration path during the entire 30 min in the open field. Quantification of the distance moved across 5-min time bins (**G**), the 30-min period (**H**), and time spend in the center zone (**I**). Values are means  $\pm$  SEM. ( $n = 10$  mice per group). Student's  $t$ -test. \*\*\* $p < 0.001$ , ### $p < 0.001$  for novel mouse vs. novel object; SSS $p < 0.001$  for KO group vs. WT group. "ns" indicates no statistical significance

#### mPFC SOM interneurons are blunted activated during social interaction deficits in *Magel2*-null animals

To further monitor the real-time activity of mPFC SOM interneurons in *Magel2* KO animals in a three-chamber sociability assay, we injected AAVs encoding Cre-inducible calmodulin based genetically encoded GFP calcium indicators (GCaMP7s) into mPFC of SOM-Cre/*Magel2* KO mice and implanted an optic fiber above the injection site. The percentage of SOM interneurons transduction

reached  $98.08 \pm 0.42\%$  ( $n = 10$ ) at 3 weeks post-AAV injection, but a low variability was observed between mice (values ranging from 95.60 to 99.80%). The percentage of SOM interneurons transfected in each mouse was 98.55%, 98.78%, 99.62%, 95.46%, 97.36%, 96.67%, 99.63%, 97.67%, 98.21% and 98.81%, respectively.

Using fiber photometry, we recorded the population activity of mPFC SOM interneurons during social interaction (Fig. 3A-C). As illustrated in Fig. 3D, a minimal



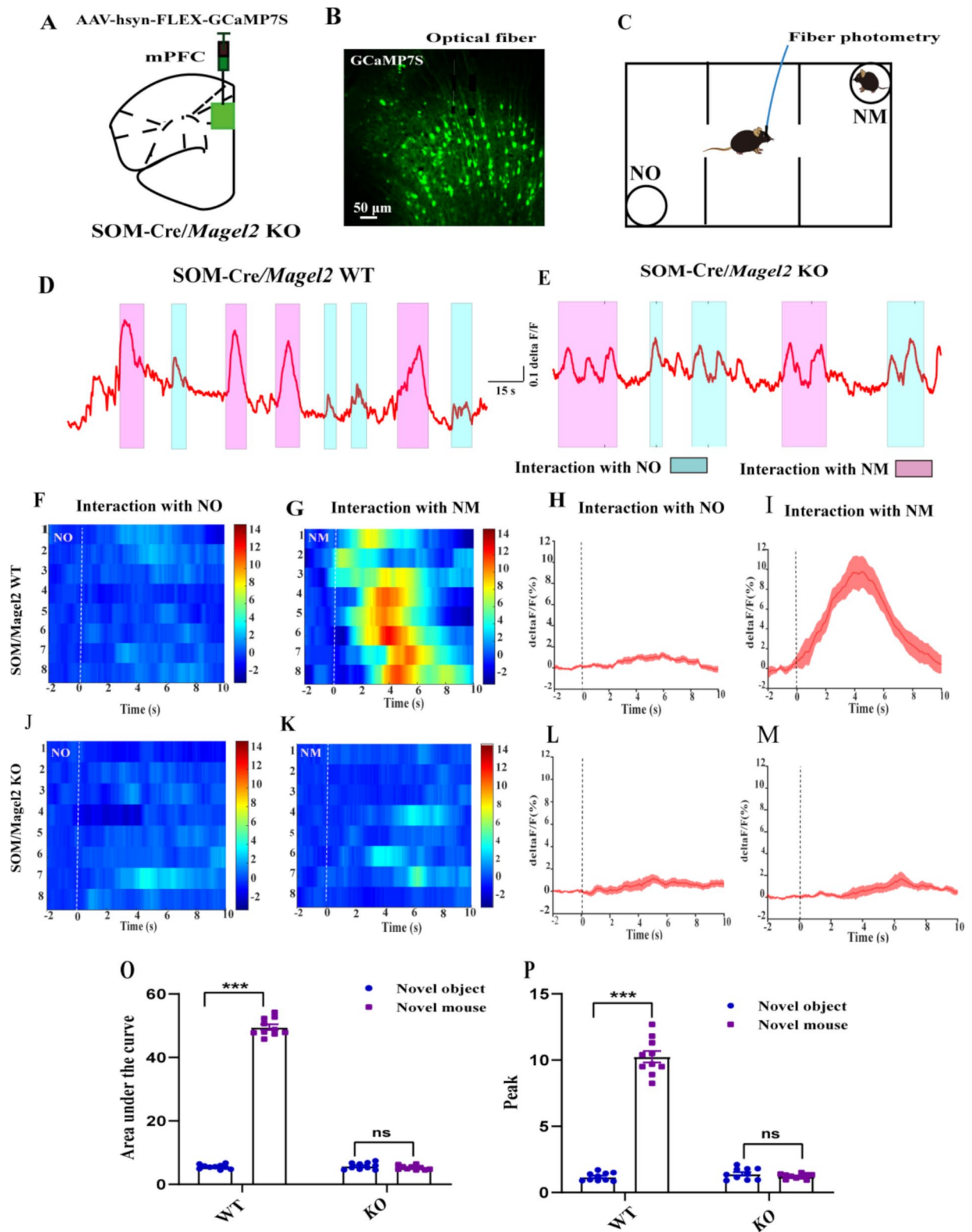


**Fig. 3** (See legend on next page.)

(See figure on previous page.)

**Fig. 3** mPFC SOM interneurons are blunted activated during social interaction in SOM-Cre/*Magel2* KO mice. **A** Schematic diagram of the fiber photometry setup. Calcium transients were recorded from GCaMP7s-positive SOM interneurons of mice subjected to the three-chamber social interaction task. **B-C** Viral strategy (**B**) and histological verification (**C**) for fiber photometry recordings of mPFC SOM interneurons. **D-E** GCaMP7s signals of SOM interneurons during the bouts of social interaction with novel object (light blue) or novel mouse (pink) in the three-chamber test. Calcium signals of a SOM-Cre/*Magel2* WT mouse showed the minimal increase to interact with the novel object. **F** The heatmap display of calcium signals was aligned to the start of individual interactions. Note that time 0 was considered as the time point when the experimental animal was closest to the novel object. Each row indicates one bout, and a total of eight bouts are shown. **H** Representative line of the peri-event plot of the averaged calcium signals. **G, I** The same as F, H but for novel mouse interaction. **J-M** Heat maps (**J, K**) and per-bout stacked plots (**L, M**) of SOM-GCaMP7s signals were the same as F and G but for SOM-Cre/*Magel2* KO. **O, P** Statistical comparison of fluorescence signals (**O**: Area under the curve; **P**: Peak amplitude) of mPFC SOM interneurons between novel object interaction and novel mouse interaction. All results are presented as means  $\pm$  SEM.  $n = 10$  animals per group. \*\*\* $p < 0.001$  for novel mouse vs. novel object

increase in calcium signals, indicative of neuronal activity, was observed when *Magel2* WT mice interacted with a novel object. As a comparison, there was a robust increase in fluorescence signals each time these experimental mice interacted with a novel mouse. The elevated SOM interneuronal activity could be seen from representative calcium trace (Fig. 3D), heatmap (Fig. 3F, G), and per-bout stacked plots (Fig. 3H, I) of SOM interneurons in *Magel2* WT mice during social interaction test. In striking contrast, only a slight change in fluorescence signals was observed when the *Magel2* KO mice interacted with either a novel object or a novel mouse (Fig. 3E, J-M). Indeed, the area under curve (AUC) of calcium signals of SOM neurons of *Magel2* WT mice during social interaction with a novel mouse were significantly increased in response to the novel mouse (NM) relative to the unfamiliar object (NO) (NO =  $5.54 \pm 0.22$ ,  $n = 10$ ; NM =  $49.55 \pm 0.87$ ,  $n = 10$ ;  $p < 0.001$ , Fig. 3O). Similar results were observed in peak amplitude (NO =  $1.19 \pm 0.1$ ,  $n = 10$ ; NM =  $10.25 \pm 0.43$ ,  $n = 10$ ;  $p < 0.001$ , Fig. 3P). We did not detect the differences in AUC (NO =  $5.77 \pm 0.32$ ,  $n = 10$ ; NM =  $5.27 \pm 0.20$ ,  $n = 10$ ;  $p = 0.21$ , Fig. 3O) and peak values (NO =  $1.42 \pm 0.13$ ,  $n = 10$ ; NM =  $1.24 \pm 0.06$ ,  $n = 10$ ;  $p = 0.24$ , Fig. 3P) of fluorescence signals measured with calcium indicators of *Magel2* KO mice. On the basis of these data, we suggest that reduced SOM interneuron activities in vivo were involved in social deficiencies of *Magel2*-deficient mice.

#### Chemogenetic inhibition of mPFC SOM neurons mimics social deficits in *Magel2* WT mice

It was widely accepted that abnormal hypoactivity of a subpopulation of GABAergic cells in mPFC is associated with impairments in social interaction [39]. Consistently, our electrophysiological recordings revealed a reduced firing rate in mPFC SOM interneurons during social deficits (Fig. 2). To determine whether the reduced excitability of SOM interneurons was involved in social impairments, we employed a pharmacogenetic approach to inactivate SOM neurons during social deficits. In specific, SOM-Cre/*Magel2* WT mice were bilaterally infected with AAV9-DIO-hM4Di-mCherry (treatment group) or AAV9-DIO-mCherry (control group) in the

mPFC. Approximately  $97.58 \pm 0.48\%$  of SOM-expressing neurons were hM4Di-mCherry positive, indicative of high efficiency of viral targeting for SOM neurons ( $n = 8$ , Fig. 4A, B). The proportion of hM4Di-mCherry-positive neurons which tested negative for SOM in each experimental mouse as follows: 2.37%, 3.52%, 3.42%, 2.76%, 3.26%, 4.06%, 3.74%, 2.96%, respectively. Hu et al., demonstrated that Cre could be expressed by a small and varying population of parvalbumin interneurons in the SOM-Cre mouse line [40]. Consistent with previous findings, in the current study the percentage of hM4Di-mCherry-containing cells that expressed parvalbumin in each mouse was 2.58%, 2.79%, 3.32%, 3.13%, 2.85%, 1.94%, 2.64%, 3.06%, 1.87% and 2.62%, respectively.

In addition, the percentage of SOM interneurons transduction reached  $97.07 \pm 0.39\%$  ( $n = 10$ ), but a low variability was detected between mice (values ranging from 94.56 to 98.67%). The percentage of SOM interneurons transfected in each mouse was 96.84%, 95.64%, 97.85%, 98.67%, 97.79%, 96.75%, 97.84%, 96.86%, 94.56% and 97.89%, respectively.

To verify the effectiveness of pharmacogenetic inactivation, we directly evaluated the effect of CNO on SOM interneurons firing in vivo in mice implanted with tetrodes. As predicted, the spike rates of SOM neurons decreased significantly following CNO administration (hM4Di =  $27.00 \pm 0.77$  Hz,  $n = 17$  neurons from 6 mice; mCherry =  $11.59 \pm 0.45$  Hz;  $n = 17$  neurons from 5 mice;  $p < 0.001$ , Fig. 4C, D).

Next, we measured social behavior following CNO administration with a three-chamber social interaction test (Fig. 4E). As seen in Fig. 4F-H, mice expressing mCherry displayed a significant increase in the time spent in the compartment containing a novel mouse relative to the empty chamber (NO =  $199.70 \pm 3.99$  s,  $n = 10$ ; NM =  $253.40 \pm 4.06$  s,  $n = 10$ ;  $p < 0.001$ ). In contrast, this was not true for the CNO + hM4Di group (NO =  $192.30 \pm 6.18$  s,  $n = 10$ ; NM =  $194.40 \pm 5.10$  s,  $n = 10$ ;  $p = 0.80$ ).

Furthermore, the AAV-mCherry administered mice spent remarkably more time sniffing the novel mouse compared to the novel object (NO =  $83.90 \pm 3.72$  s,  $n = 10$ ; NM =  $155.60 \pm 2.65$  s,  $n = 10$ ;  $p < 0.001$ ). Mice

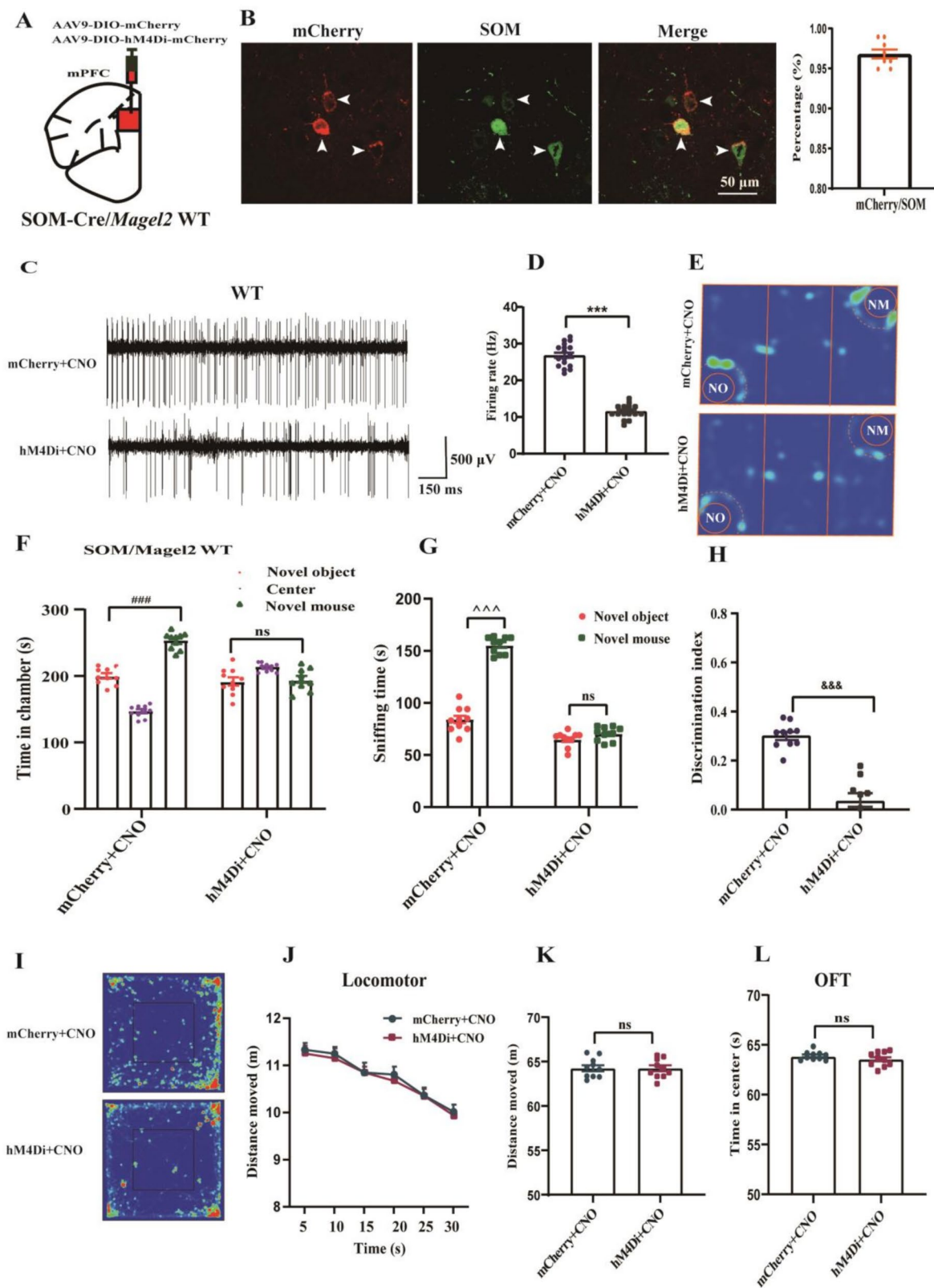


**Fig. 4** (See legend on next page.)

(See figure on previous page.)

**Fig. 4** Inhibition of SOM neuronal activity of the mPFC mimics social defects in SOM-Cre/*Magel2* WT mice. **A** Cartoon of the injection of recombinant AAV virus. **B** Neurons in the mPFC infected with AAV-DIO-hM4Di-mCherry (red) co-stained with SOM-expressing interneurons (green). Quantification of specificity of hM4Di-mCherry to label SOM interneurons ( $n=8$  per group). **C** Example recording of spontaneous spikes from a SOM interneuron before (top) and after CNO administration (bottom). **D** statistics of SOM firing rates before and after CNO administration ( $n=17$  cells in 6 mice for each group). **E** Representative heat map displaying the locations of an mCherry-expressing control animal (top) and an hM4Di-expressing mouse (bottom) in the three-chamber test following CNO administration. **F** Quantification of time spent by mCherry and hM4Di mice in each compartment. mCherry mice spent significantly more time in the compartments of the unfamiliar animal relative to the novel object. No dramatic difference in the time spent exploring the compartment containing the novel animal relative to the time spent exploring the novel object for hM4Di mice. **G** mCherry mice spent more time sniffing the unfamiliar animal compared with the novel object. The hM4Di mice spent similar time sniffing with the novel mouse and the novel object. **H** Social interaction index was significantly lower in hM4Di mice. Sample size of 10 in **F, G, H** was calculated. **I** Sample path recordings during the entire 30-min period in the open field test. **J** The locomotor activities of the control (mCherry) and hM4Di-expressing animal at 5-min intervals were evaluated 30 min after CNO injection. Quantification of the total distance moved (**K**) and the amount of time spent in the arena's center (**L**). Sample size of 10 in **J, K, L** was determined. Data are presented as mean  $\pm$  SEM. One-way ANOVA with Tukey's post hoc test. Unpaired Student's *t*-test. \*\*\*\* $p < 0.001$ , <sup>SS</sup> $p < 0.001$ , compared to mCherry group; <sup>###</sup> $p < 0.001$ , <sup>^^^</sup> $p < 0.001$  for novel mouse vs. novel object; "ns" indicates not significantly different

expressing hM4Di did not exhibit any particular preference, in accordance with a lack of interest in the unfamiliar animal (NO =  $65.30 \pm 2.28$  s,  $n=10$ ; NM =  $70.50 \pm 2.13$  s,  $n=10$ ;  $p=0.11$ ). The AAV-hM4Di group had a significantly lower discrimination index than the control mice (mCherry =  $0.30 \pm 0.02\%$ ,  $n=10$ ; hM4Di =  $0.04 \pm 0.03\%$ ,  $n=10$ ;  $p < 0.001$ ). In the open-field test, the CNO caused behavioral changes were unlikely to derive from altered general activity or anxiety (WT =  $0.44 \pm 0.02$ ,  $n=10$ ; KO =  $0.02 \pm 0.02$ ,  $n=10$ ;  $p=0.001$ ), as the hM4Di-expressing animals exhibited locomotor activity in 5 min intervals [at 5 min, mCherry =  $11.32 \pm 0.13$ ,  $n=10$ ; hM4Di =  $11.25 \pm 0.17$ ,  $n=10$ ;  $p=0.72$ ; at 10 min, mCherry =  $11.24 \pm 0.15$ ,  $n=10$ ; hM4Di =  $11.14 \pm 0.22$ ,  $n=10$ ;  $p=0.72$ ; at 15 min, mCherry =  $10.84 \pm 0.20$ ,  $n=10$ ; hM4Di =  $10.84 \pm 0.13$ ,  $n=10$ ;  $p=0.10$ ; at 20 min, mCherry =  $11.80 \pm 0.16$ ,  $n=10$ ; hM4Di =  $11.66 \pm 0.16$ ,  $n=10$ ;  $p=0.56$ ; at 25 min, mCherry =  $10.36 \pm 0.17$ ,  $n=10$ ; hM4Di =  $10.35 \pm 0.13$ ,  $n=10$ ;  $p=0.97$ ; at 30 min, mCherry =  $10.01 \pm 0.14$ ,  $n=10$ ; hM4Di =  $9.93 \pm 0.24$ ,  $n=10$ ;  $p=0.79$ ], total distance (mCherry =  $11.32 \pm 0.13$ ,  $n=10$ ; hM4Di =  $11.25 \pm 0.17$ ,  $n=10$ ;  $p=0.25$ ), and time spent in the center (mCherry =  $63.93 \pm 0.14$ ,  $n=10$ ; hM4Di =  $63.61 \pm 0.22$ ,  $n=10$ ;  $p=0.72$ ), similar to those of the AAV-mCherry group (Fig. 4I-L). Together, these results therefore revealed that suppression of mPFC SOM neurons reduces social interaction in *Magel2* WT mice.

#### Optogenetic activation of mPFC SOM interneurons rescues social impairment in *Magel2* KO mice

Since the association between mPFC SOM neuron hypoactivity and social impairments in *Magel2* WT mice, we tested whether the activation of SOM neurons was sufficient to alleviate social impairments. We selectively activated mPFC SOM neurons by delivering blue light in SOM-Cre and *Magel2* KO double-transgenic mice unilaterally infected in the mPFC with AAV-DIO-ChR2-mCherry or AAV-DIO-mCherry. Around  $96.16 \pm 0.61\%$  of SOM-containing interneurons were ChR2-mCherry positive ( $n=8$ , Fig. 5A, B). The proportion of

ChR2-mCherry-positive cells which tested negative for SOM in each experimental mouse was as follows: 3.76%, 2.87%, 3.56%, 4.06%, 3.59%, 2.87%, 3.35%, and 2.71%, respectively. The percentage of ChR2-mCherry-containing neurons that expressed parvalbumin in each mouse was 2.64%, 3.41%, 2.21%, 1.50%, 3.38%, 2.79%, 2.94%, 3.12%, 2.75% and 1.36%, respectively.

Additionally, the percentage of SOM interneurons transduction reached  $96.52 \pm 0.52\%$  ( $n=10$ ), but a low variability was observed between mice (values ranging from 93.79 to 98.64%). The percentage of SOM interneurons transfected in each mouse was 98.57%, 96.78%, 97.62%, 93.79%, 97.45%, 95.71%, 96.73%, 94.48%, 95.38% and 98.64%, respectively.

We used electrophysiology recordings to ascertain the efficacy of neuronal activity under optogenetic activation (20 Hz, 10 ms pulse, laser 473 nm) of SOM neurons in mPFC (mCherry =  $12.10 \pm 0.83$  Hz,  $n=15$  neurons from 6 mice; ChR2 =  $23.80 \pm 0.82$  Hz;  $n=15$  neurons from 5 mice;  $p < 0.001$ ; Fig. 5C-D).

In social interaction and three-chamber test, optogenetic activation of mPFC SOM neurons in *Magel2* KO mice accompanied by more time spent in the compartment of the novel mouse relative to that of the unfamiliar object (NO =  $140.30 \pm 4.40$  s,  $n=10$ ; NM =  $319.70 \pm 3.52$  s,  $n=10$ ;  $p < 0.001$ , Fig. 5F). No corresponding differences were detected in the amount of time spent exploring these two compartments in AAV-mCherry group (NO =  $235.20 \pm 3.48$  s,  $n=10$ ; NM =  $224.60 \pm 3.76$  s,  $n=10$ ;  $p=0.05$ , Fig. 5F). Moreover, ChR2 injection in *Magel2* KO was associated with mice having spent more time interacting with the unfamiliar mouse relative to the unfamiliar object (NO =  $73.6 \pm 3.77$  s,  $n=10$ ; NM =  $140.30 \pm 6.34$  s,  $n=10$ ;  $p < 0.001$ , Fig. 5G). In contrast, mCherry group spent a similar amount of time sniffing the novel animal and the familiar mouse (NO =  $58.60 \pm 2.08$  s,  $n=10$ ; NM =  $65.50 \pm 1.96$  s,  $n=10$ ;  $p=0.19$ , Fig. 5G). The AAV-ChR2 group had a significantly higher discrimination index than the control mice (mCherry =  $0.03 \pm 0.02\%$ ,  $n=10$ ; ChR2 =  $0.41 \pm 0.02\%$ ,  $n=10$ ;  $p < 0.001$ , Fig. 5H).

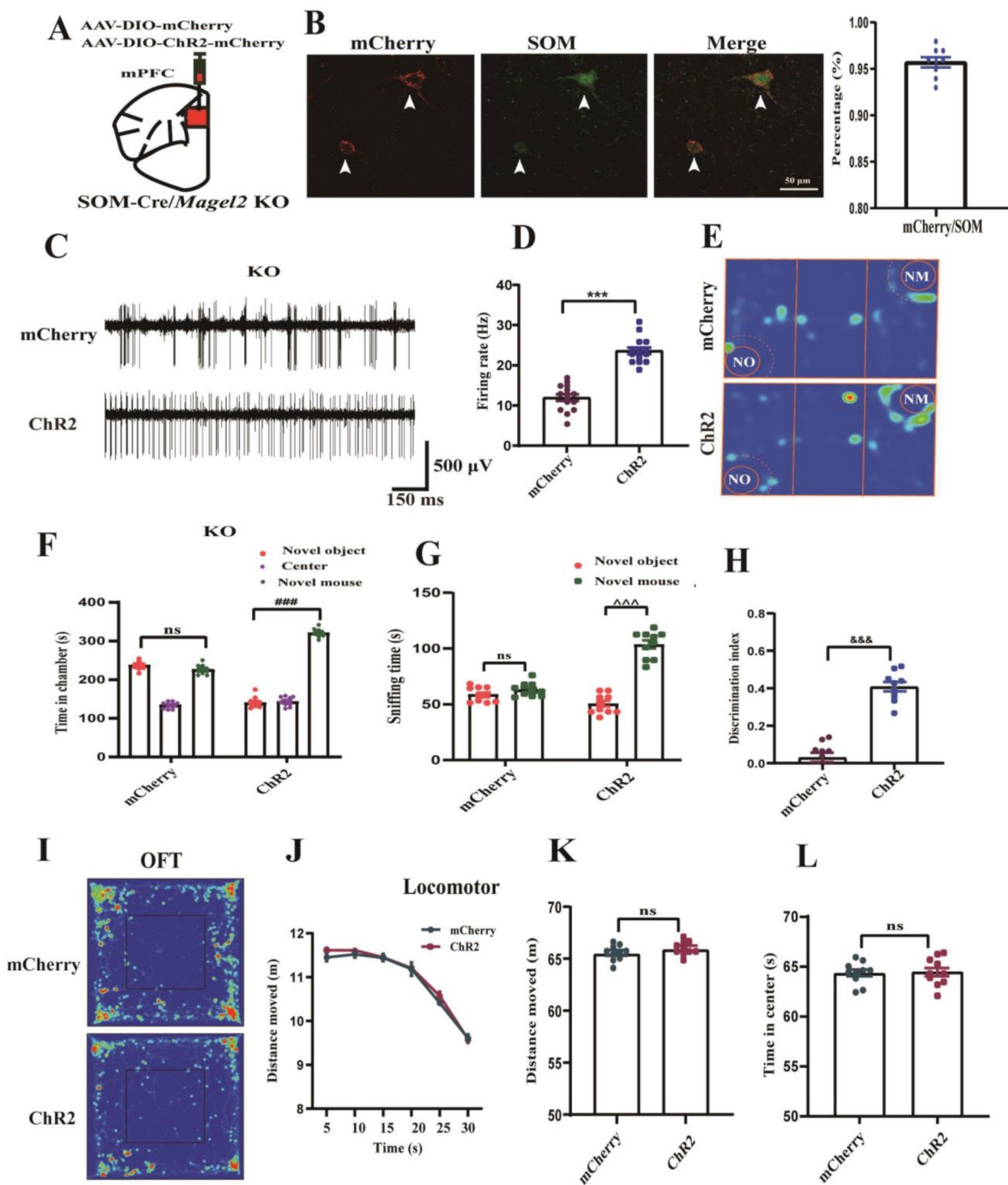


**Fig. 5** (See legend on next page.)

The open field test data revealed no significant changes in locomotor activity in 5 min intervals [at 5 min, mCherry =  $11.45 \pm 0.08$ ,  $n = 10$ ; ChR2 =  $11.61 \pm 0.7$ ,  $n = 10$ ;  $p = 0.16$ ; at 10 min, mCherry =  $11.52 \pm 0.09$ ,  $n = 10$ ; ChR2 =  $11.60 \pm 0.04$ ,  $n = 10$ ;  $p = 0.44$ ; at 15 min,

mCherry =  $11.44 \pm 0.09$ ,  $n = 10$ ; ChR2 =  $11.45 \pm 0.09$ ,  $n = 10$ ;  $p = 0.95$ ; at 20 min, mCherry =  $11.18 \pm 0.16$ ,  $n = 10$ ; ChR2 =  $11.21 \pm 0.04$ ,  $n = 10$ ;  $p = 0.88$ ; at 25 min, mCherry =  $10.41 \pm 0.03$ ,  $n = 10$ ; ChR2 =  $10.57 \pm 0.10$ ,  $n = 10$ ;  $p = 0.15$ ; at 30 min, mCherry =  $9.61 \pm 0.09$ ,  $n = 10$ ;

(See figure on previous page.)

**Fig. 5** Optogenetic stimulation of mPFC SOM interneurons rescues the social deficiency in SOM-Cre/*Magel2* KO mice. **A** Cartoon showing the injection of AAV virus. **B** Neurons in the mPFC infected with AAV-DIO-ChR2-mCherry (red) co-stained with SOM interneurons (green). Quantification of specificity of ChR2-mCherry to label SOM interneurons ( $n=8$  per group). **C** Sample traces of in vivo photo-tagged single unit spike recordings before (top) and after ChR2-optogenetic stimulation (bottom). **D** Statistics of SOM firing rates before and after ChR2-optogenetic stimulation ( $n=15$  neurons from 6 mice). **E** Representative movement traces showing the locations of an mCherry-expressing control mouse (top) and a ChR2-containing mouse (bottom) in the three-chamber social test. **F** Quantification of time spent by mCherry and ChR2-treated mice in each chamber. ChR2 mice spent more time exploring the chamber containing the novel animal relative to novel object. In contrast, no significant difference in the time spent exploring the compartment containing the novel animal as compared to the time spent exploring the unfamiliar object for mCherry mice. **G** ChR2-injected mice spent significantly more time sniffing and engaging with the novel mouse as compared with the unfamiliar object. In contrast, mCherry mice spent equal amounts of time sniffing the novel mouse and unfamiliar object. **H** Social interaction index was significantly higher in ChR2 mice. Sample size of 10 in **F**, **G**, and **H** was calculated. **I** Example path recordings during the entire 30 min of the open field test. Quantification of the distance moved for 5-min time bins (**J**), the total 30-min period (**K**), and time spent by AAV-ChR2 mice in the center region (**L**). Sample size of 10 in **J**, **K**, and **L** was determined. Results are presented as mean  $\pm$  SEM. One-way ANOVA with Tukey's post hoc test. Unpaired Student's *t*-test. \*\*\* $p < 0.001$ , <sup>SS</sup> $p < 0.001$ , compared to mCherry group;  $\wedge\wedge\wedge p < 0.001$  for novel mouse vs. novel object; "ns" shows not significantly different

ChR2 =  $9.58 \pm 0.08$ ,  $n=10$ ],  $p=0.83$ ], total distance (mCherry =  $65.62 \pm 0.24$ ,  $n=10$ ; ChR2 =  $66.03 \pm 0.21$ ,  $n=10$ ;  $p=0.21$ ), and in the time spent in the center (mCherry =  $64.32 \pm 0.36$ ,  $n=10$ ; ChR2 =  $64.45 \pm 0.44$ ,  $n=10$ ;  $p=0.001$ ), suggesting anxiety-negative behaviors (Fig. 5I-L). These results further confirms that activation of mPFC SOM interneurons is sufficient to mitigate social impairment in *Magel2* KO mice.

#### Activation of SOM neurons in the mPFC-LS pathway rescues social impairments in *Magel2*-deficient animals

The mPFC and LS are extensively interconnected and both contribute to the modulation of social behaviors [14]. To determine whether the mPFC<sup>SOM</sup>-LS pathway mediates social behaviors, we bilaterally injected the AAV carrying Cre-dependent AAV2-retro-DIO-EGFP or control EGFP into the LS of SOM-Cre/*Magel2* KO mice. Three weeks after this operation, the percentage of SOM interneurons transduction reached  $97.05 \pm 0.38\%$  ( $n=10$ ), but a low variability was observed between mice (values ranging from 95.32 to 98.67%). The percentage of SOM interneurons transfected in each mouse was 98.67%, 96.84%, 98.51%, 98.38%, 97.65%, 96.47%, 96.46%, 95.68%, 95.32% and 96.49%, respectively.

We found the mPFC SOM-expressing axon terminals projected to the neurons in the LS (Fig. 6A-B). To further confirm that LS received functional GABAergic projections from mPFC SOM-positive neurons in SOM-Cre/*Magel2* KO mice, we recorded blue light-evoked IPSCs (eIPSCs) in neurons in the LS when optogenetically activating the axonal terminals in the mPFC-LS pathway in brain slices as shown in Fig. 6C-E. The eIPSCs were fully blocked by the voltage-gated sodium channel blocker TTX (ACSF =  $258.93 \pm 7.12$  s,  $n=14$  neurons from 6 mice; TTX =  $0.51 \pm 0.05$  s,  $n=14$  neurons from 6 mice;  $p < 0.001$ ), but were rescued by application of the voltage-gated potassium channel blocker 4-AP (TTX =  $0.51 \pm 0.05$  s,  $n=14$  neurons from 6 mice; TTX + 4-AP =  $249.57 \pm 5.11$  s,  $n=14$  neurons from 6 mice;  $p < 0.001$ ). Additionally, the eIPSCs were completely abolished by the GABA<sub>A</sub> receptor antagonist

PTX (TTX + 4-AP =  $249.57 \pm 5.11$  s,  $n=14$  neurons from 6 mice; PTX =  $0.46 \pm 0.05$  s,  $n=14$  neurons from 6 mice;  $p < 0.001$ ). These results demonstrated direct monosynaptic GABAergic projections from SOM-containing interneurons in the mPFC to the LS.

To determine whether the mPFC<sup>SOM</sup>-LS pathway mediates social behaviors, we activated this specific pathway by injecting the AAV-DIO-ChR2, or mCherry as control, bilaterally into the mPFC and bilaterally implanted an optical fiber above the LS in SOM-Cre/*Magel2* KO mice. As seen in Fig. 6F-I, we found that when the mPFC<sup>SOM</sup>-LS pathway was photoactivated, the *Magel2* KO mice spent significantly more time in the compartment of the stranger mouse relative to the unfamiliar object (NO =  $184.10 \pm 4.67$  s,  $n=10$ ; NM =  $297.4 \pm 6.55$  s,  $n=10$ ;  $p < 0.001$ ; Fig. 6G). In contrast, administration of mCherry treatment was linked to these animals having spent equal amounts of time in the chamber containing the novel mouse and the novel object (NO =  $212.20 \pm 3.94$  s,  $n=10$ ; NM =  $210.90 \pm 5.91$  s,  $n=10$ ;  $p=0.99$ , Fig. 6G). In the sociability test analyzing interaction time, optogenetic activation of ChR2-expressing axonal terminals in the mPFC induced more time sniffing the novel mouse relative to the stranger object (NO =  $65.2 \pm 2.52$  s,  $n=10$ ; NM =  $113.10 \pm 2.45$  s,  $n=10$ ;  $p < 0.001$ ; Fig. 6H). The mCherry-exposed mice spent similar amounts of time interacting with the novel mouse and the unfamiliar object (NO =  $54.90 \pm 2.29$  s,  $n=10$ ; NM =  $58.20 \pm 2.42$  s,  $n=10$ ;  $p=0.34$ , Fig. 6H). The optogenetic activation of mPFC<sup>SOM</sup>-LS pathway also induced a significantly higher discrimination index than the mCherry group (mCherry =  $0.03 \pm 0.01\%$ ,  $n=10$ ; ChR2 =  $0.27 \pm 0.07\%$ ,  $n=10$ ;  $p < 0.001$ , Fig. 6I). Together, these data showed that SOM-positive neurons in the mPFC form functional inhibitory connections with neurons in the LS, and activating the mPFC<sup>SOM</sup>-LS pathway can rescue social impairments of the *Magel2* KO mice.

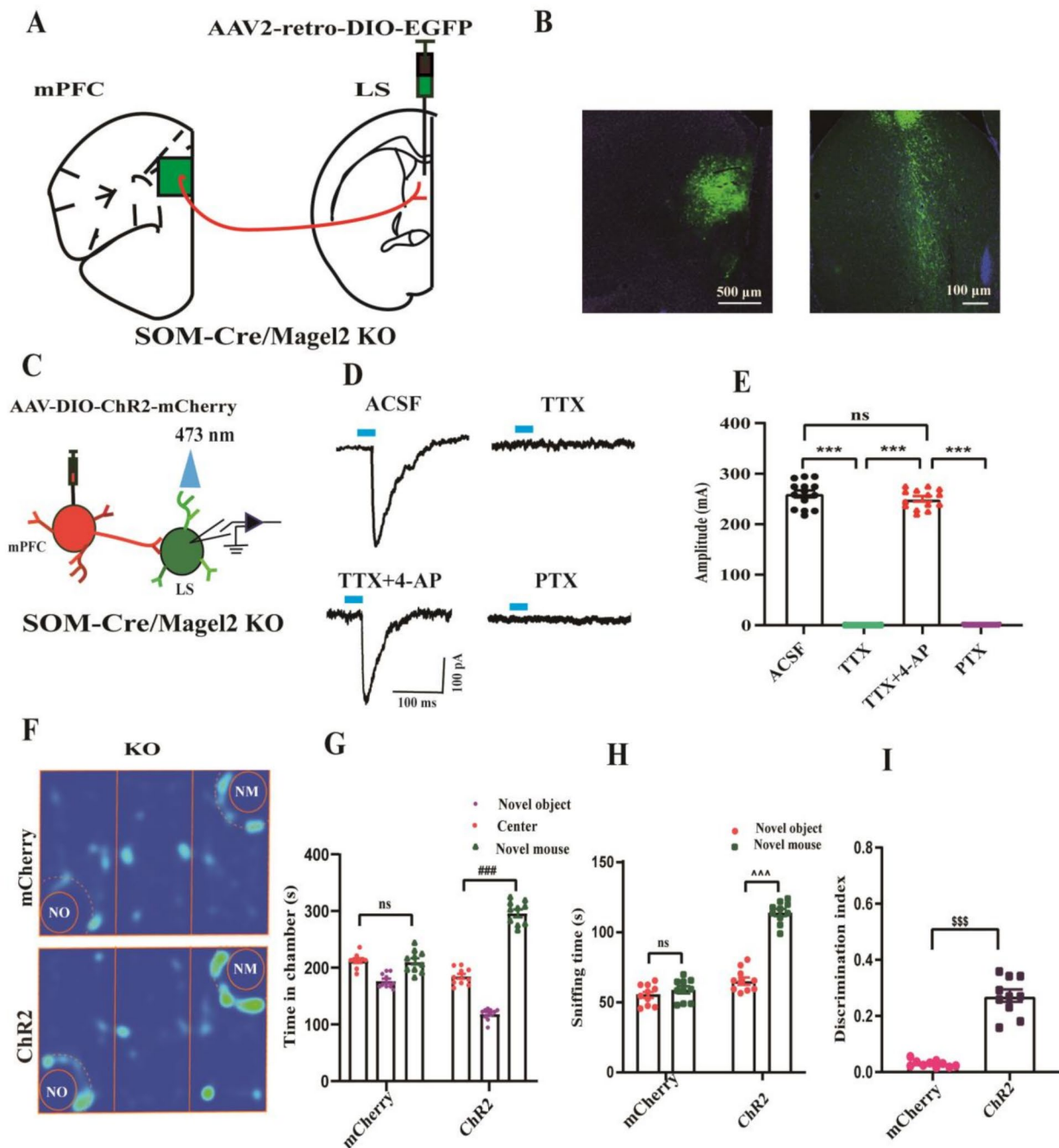


**Fig. 6** Activation of monosynaptic projection from SOM-positive neurons in the mPFC to LS mitigates social deficits in SOM-Cre/*Magel2* KO mice. **A** Schematic of viral injection for retrograde tracing from LS in KO mice. **B** (Left) Representative images displaying retro-AAV injection sites in LS (green). (Right) Fluorescence images of mPFC showing the retrograde labeled LS-projecting cells (in green). **C** Schematic showing the configuration for electrophysiological recording of the mPFC<sup>SOM</sup>-LS projection. **D, E** Representative traces (**D**) and statistical analysis (**E**) of optogenetic stimulation evoked IPSCs in LS neurons in ACSF and following sequential application of TTX (1  $\mu$ M/L), TTX + 4-AP (100  $\mu$ M/L) and PTX (50  $\mu$ M/L), respectively. Blue bar indicated optogenetic light stimulation ( $n = 14$  neurons from 6 mice). **F-I** Representative heatmaps (**F**) and statistical analysis (**G-I**) of optogenetic activation of SOM-positive neurons in the rostral mPFC-LS pathway in the open field test in the mCherry (top) and Chr2 (bottom) groups. Sample size of 10 in **G, H, I** was calculated. All results are presented as mean  $\pm$  SEM. One-way ANOVA with Tukey's post hoc test. Unpaired Student's *t*-test. \*\*\*\* $p < 0.001$ ; ### $p < 0.001$ , ^^^ $p < 0.001$  for novel mouse vs. novel object; ^^^ $p < 0.001$ , compared to mCherry group; "ns" indicates not significantly different

## Discussion

In our study, we found that reduced intrinsic excitability and hypoactivation of mPFC SOM interneurons in *Magel2*-null mice is involved in social interaction deficits. Noticeably, inhibition of SOM excitability in the mPFC can cause social impairments. Further, the enhanced social behaviors induced optogenetic activation by mPFC SOM interneurons or monosynaptic inhibitory connections of mPFC<sup>SOM</sup>-LS. Overall, our data provide direct evidence for the functional effect of the mPFC<sup>SOM</sup>-LS neural circuit on social impairments in *Magel2* mouse model of ASD.

Hallmark symptoms of ASD encompass deficits in social behaviors [1, 32]. Mice are a highly social species that exhibit strong responses to novel conspecifics. The three-chamber social interaction task, which evaluates the amount of time a mouse spends in close proximity with another animal, was developed and validated to measure sociability [14]. Previous literature shows that *Magel2*-deficient mice recapitulate autistic-like symptoms, including abnormal social behaviors [3, 6]. With the three-chamber social behavior test, our investigation further demonstrated that animals lacking *Magel2* displayed social behavioral disturbances, which are key characteristics of ASD.

Multiple lines of evidence implicate blunted neuronal excitability in the genetically engineered and idiopathic ASD mouse models and strongly relate to sociability impairments [41–43]. We attempted to investigate whether intrinsic neuronal excitability SOM-expressing interneurons in *Magel2*-null are influenced. We observed that deficiency of *Magel2* was associated with decreased action potential discharge frequencies of mPFC SOM neuron in response to depolarization inputs of SOM neurons in slices via whole-cell patch-clamp recordings. Mice with deletion of *Magel2* gene also exhibited enhanced the threshold current. Following this line of reasoning, we conclude that these changes inhibited SOM-positive neurons' excitability.

The genetically encoded calcium fluorescent indicators allowed us to simultaneously record the activity of neural populations in animals by in vivo fiber photometry [44]. Subsequently, we injected Cre-dependent AAV expressing GCaMP7s into the mPFC and carried out fiber photometry. We found the pronounced augmentation in GCaMP7s fluorescence intensity of SOM-expressing interneurons that was elicited in *Magel2* WT mice during social interaction in the three-chamber test. By contrast, no significant differences in the area under the curve or the amplitude of calcium signals in SOM-expressing cells were observed in *Magel2*-deficient mice when they explored a novel conspecific and a novel object. In conjunction with our results, animals with an *Auts2* knockout-closely associated with ASD-also

exhibited comparable moderate calcium transients when investigating Stranger 1 and Stranger 2, indicating deficits in social recognition [45]. Collectively, these findings suggest that diminished SOM interneuron activity in vivo may contribute to the sociability impairments observed in *Magel2*-null animals.

We further show that chemogenetic inhibition of mPFC SOM neurons reduced social interactions. These sociability deficits can be rescued by optogenetic activation of mPFC SOM interneurons in *Magel2* KO mice. In agreement with our results, loss of forkhead box G1 (*Foxg1*) impairs the development of cortical SOM interneurons resulting in aberrant emotional and social behaviors [46]. Notably, a recent study indicated selective aryl hydrocarbon receptor nuclear translocator 2 (*ARNT2*) ablation in SOM-expressing interneurons in anterior cingulate cortex leads to reduced pyramidal cell excitability and enhances spontaneous firing resulting in reduced affective empathy [12]. Similarly, Scheggia et al., uncovered that inhibition of mPFC SOM interneurons abolishes affective state discrimination. Synchronized activation of mPFC SOM interneurons induces social discrimination [20]. Consistent with previous views, our results demonstrate an essential role for SOM interneurons action in the mPFC in social behaviors. Optogenetic manipulation of mPFC SOM can ameliorate social impairments in *Magel2* KO animals.

The mPFC mediates social behaviors through output connections with LS [14, 22]. Reyes et al., demonstrated that the release of neuropeptide corticotropin-releasing hormone in the mPFC during familiar encounters disinhibits rostral LS neurons, thereby contributing to social novelty preference [22]. Li et al., identified that chemogenetic inhibition of LS neurotensin neurons increased social investigation time following chronic social defeat stress [24]. Similarly, Bredewold et al., showed that bicuculline-induced blockade of GABA<sub>A</sub> receptors in the LS decreased social play behaviors [26]. Intriguingly, we identified monosynaptic circuit from GABAergic axon projection of SOM-positive neurons in the mPFC to LS. Optogenetic stimulation of the mPFC<sup>SOM</sup>-LS GABAergic pathway attenuates social deficits in mice lacking *Magel2* related to ASD.

In a complementary fashion, three chamber sociability task was used to measure sociability, or the propensity to engage in social interaction [47]. For instance, 5-HT release in nucleus accumbens reverses social deficits in 16p11.2 deletion mouse model of ASD [48]. In social novelty task, mice show a preference for interacting with the novel mouse compared to the familiar mouse, which can be tested in the second phase of three-chamber social behavioral test. Impairments in the task are used to infer deficits in social memory [47, 49]. Further researches are required to more specifically target

whether mPFC<sup>SOM</sup>-LS pathway is implicated in social memory in *Magel2*-deficient animals.

## Conclusions

To sum up, the present study demonstrated that reduced intrinsic excitability and hypoactivity of prefrontal SOM interneurons in *Magel2*-deficient mice implicated in social defects. Activation of the excitability of SOM in the mPFC and mPFC<sup>SOM</sup>-LS pathway can both promote sociability of *Magel2*-null mice. Our findings expand our understanding regarding the function of mPFC region and complement the existing neural networks underlying social impairments in *Magel2* animal model of ASD. Besides, these data indicate that mPFC SOM interneurons and mPFC<sup>SOM</sup>-LS inhibitory projections are potential therapeutic targets for ameliorating social behavioral disturbances often observed in ASD.

## Author contributions

XW conceived the project, designed the experiments, and conducted manuscript writing. MC and DM performed immunostaining, fiber photometry recordings, and data analysis. XW carried out patch clamp electrophysiology and in vivo optrode recording data analysis. XW, CG and QW conducted optogenetic and chemogenetic manipulation. SS, JG and SZ carried out behavioral assays. XY, HZ and YW did confocal imaging. GB and YZ contributed to the scientific discussion and were responsible for funding acquisition. All authors supervised and approved the submitted version of the manuscript.

## Funding

This work was supported by the Scientific and Technological Project of Henan (232102311006), Medical Science and Technique Program of Henan (LHGJ20240546, LHGJ20220712), National Natural Science Foundation of China (81901387, 82260967), Autonomous Region Natural Science Foundation (Excellent Youth Project, 2022AAC05030), STI 2030-Major Projects (2021ZD0200500), and Autonomous Region Key Research and Development Plan-Talent Introduction Project (2021YCX0059).

## Data availability

No datasets were generated or analysed during the current study.

## Declarations

### Ethics approval and consent to participate

All animal experimental procedures were performed according to the National Institutes of Health Guide for the Care and Use of Laboratory Animals and were approved by the Animal Ethics Committee of Zhengzhou University.

### Consent for publication

Not applicable.

### Competing interests

The authors declare no competing interests.

Received: 5 October 2024 / Accepted: 19 February 2025

Published online: 11 March 2025

## References

- Luo YF, Lu L, Song HY, Xu H, Zheng ZW, Wu ZY, Jiang CC, Tong C, Yuan HY, Liu XX, et al. Divergent projections of the prelimbic cortex mediate autism- and anxiety-like behaviors. *Mol Psychiatry*. 2023;28(6):2343–54.
- Kim SW, Lee H, Song DY, Lee GH, Ji J, Park JW, Han JH, Lee JW, Byun HJ, Son JH, et al. Whole genome sequencing analysis identifies sex differences of

- Familial pattern contributing to phenotypic diversity in autism. *Genome Med*. 2024;16(1):114.
- Bertoni A, Schaller F, Tyzio R, Gaillard S, Santini F, Xolin M, Diabira D, Vaidyanathan R, Matarazzo V, Medina I, et al. Oxytocin administration in neonates shapes hippocampal circuitry and restores social behavior in a mouse model of autism. *Mol Psychiatry*. 2021;26(12):7582–95.
  - Heimdörfer D, Vorleuter A, Eschlböck A, Spathopoulou A, Suarez Cubero M, Farhan H, Reiterer V, Spanjaard M, Schaaf CP, Huber LA, et al. Truncated variants of MAGEL2 are involved in the etiologies of the Schaaf-Yang and Prader-Willi syndromes. *Am J Hum Genet*. 2024;111(7):1383–404.
  - Prato LCD, Zayan U, Abdallah D, Point V, Schaller F, Pallesi Pocachard E, Montheil A, Cnaan S, Gaiarsa JL, Muscatelli F, et al. Early life Oxytocin treatment improves thermo-sensory reactivity and maternal behavior in neonates lacking the autism-associated gene *Magel2*. *Neuropsychopharmacology*. 2022;47(11):1901–12.
  - Oztan O, Zyga O, Stafford DEJ, Parker KJ. Linking Oxytocin and arginine vasopressin signaling abnormalities to social behavior impairments in Prader-Willi syndrome. *Neurosci Biobehav Rev*. 2022;142:104870.
  - Gregorio DD, Popic J, Enns JP, Inserra A, Skalecka A, Markopoulos A, Posa L, Lopez Canul M, Qianzi H, Lafferty CK, et al. Lysergic acid diethylamide (LSD) promotes social behavior through mTORC1 in the excitatory neurotransmission. *Proc Natl Acad Sci USA*. 2021;118(5):1–9.
  - Li H, Kawatake-Kuno A, Inaba H, Miyake Y, Itoh Y, Ueki T, Oishi N, Murai T, Suzuki T, Uchida S. Discrete prefrontal neuronal circuits determine repeated stress-induced behavioral phenotypes in male mice. *Neuron*. 2024;112(5):786–804.
  - Sato M, Nakai N, Fujima S, Choe KY, Takumi T. Social circuits and their dysfunction in autism spectrum disorder. *Mol Psychiatry*. 2023;28(8):3194–206.
  - Li YX, Tan ZN, Li XH, Ma B, Nti FA, Lv XQ, Tian ZJ, Yan R, Man HY, Ma XM. Increased gene dosage of *RFWD2* causes autistic-like behaviors and aberrant synaptic formation and function in mice. *Mol Psychiatry*. 2024;29(8):2496–509.
  - Christian P, Kaiser J, Taylor PC, George M, Schütz Bosbach S, Soutschek A. Belief updating during social interactions: neural dynamics and causal role of dorsomedial prefrontal cortex. *J Neurosci*. 2024;44(22):1669232024.
  - Choi J, Jung S, Kim J, So D, Kim A, Kim S, Choi S, Yoo E, Kim JY, Jang YC, et al. *ARNT2* controls prefrontal somatostatin interneurons mediating affective empathy. *Cell Rep*. 2024;43(9):114659.
  - Godavarthi SK, Li HQ, Pratelli M, Spitzer NC. Embryonic exposure to environmental factors drives transmitter switching in the neonatal mouse cortex causing autistic-like adult behavior. *Proc Natl Acad Sci USA*. 2024;121(35):2406928121.
  - Mack NR, Bouras NN, Gao WJ. Prefrontal regulation of social behavior and related deficits: insights from rodent studies. *Biol Psychiatry*. 2024;96(2):85–94.
  - Yan Z, Rein B. Mechanisms of synaptic transmission dysregulation in the prefrontal cortex: pathophysiological implications. *Mol Psychiatry*. 2022;27(1):445–65.
  - Lee BR, Dalley R, Miller JA, Chartrand T, Close J, Mann R, Mukora A, Ng L, Alfiler L, Baker K, et al. Signature morphoelectric properties of diverse GABAergic interneurons in the human neocortex. *Science*. 2023;382(6667):6484.
  - Utashiro N, MacLaren DAA, Liu YC, Yaqubi K, Wojak B, Monyer H. Long-range inhibition from prelimbic to cingulate areas of the medial prefrontal cortex enhances network activity and response execution. *Nat Commun*. 2024;15(1):5772.
  - Riedemann T. Diversity and function of somatostatin-expressing interneurons in the cerebral cortex. *Int J Mol Sci*. 2019;20(12):1–21.
  - Joffe ME, Maksymetz J, Luschingner JR, Dogra S, Ferranti AS, Luessen DJ, Gallinger IM, Xiang Z, Branthwaite H, Melugin PR, et al. Acute restraint stress redirects prefrontal cortex circuit function through mGlu5 receptor plasticity on somatostatin-expressing interneurons. *Neuron*. 2022;110(6):1068–83.
  - Scheggia D, Managò F, Maltese F, Bruni S, Nigro M, Dautan D, Latuske P, Contarini G, Gomez Gonzalo M, Requeie LM, et al. Somatostatin interneurons in the prefrontal cortex control affective state discrimination in mice. *Nat Neurosci*. 2020;23(1):47–60.
  - Heukelum Sv, Mogavero F, Wal MAEvd, Geers FE, França ASC, Buitelaar JK, Beckmann CF, Glennon JC, Havenith MN. Gradient of parvalbumin- and somatostatin-expressing interneurons across cingulate cortex is differentially linked to aggression and sociability in BALB/cJ mice. *Front Psychiatry*. 2019;10:809.
  - Reyes NSL, Díaz PS, Nogueira R, Ruiz Pino A, Nomura Y, Solis CAd, Schulkin J, Asok A, Leroy F. Corticotropin-releasing hormone signaling from prefrontal

- cortex to lateral septum suppresses interaction with familiar mice. *Cell*. 2023;186(19):4152–71.
23. Borie AM, Dromard Y, Chakraborty P, Fontanaud P, Andre EM, François A, Colson P, Muscatelli F, Guillon G, Desarménien MG, et al. Neuropeptide therapeutics to repress lateral septum neurons that disable sociability in an autism mouse model. *Cell Rep Med*. 2024;5(11):101781.
  24. Li L, Cuttoli RD-d, Aubry AV, Burnett CJ, Cathomas F, Parise LF, Chan KL, Morel C, Yuan C, Shimo Y, et al. Social trauma engages lateral septum circuitry to occlude social reward. *Nature*. 2023;613(7945):696–703.
  25. Rodriguez LA, Kim S-H, Page SC, Nguyen CV, Pattie EA, Hallock HL, Valerino J, Maynard KR, Jaffe AE, Martinovich K. The basolateral amygdala to lateral septum circuit is critical for regulating social novelty in mice. *Neuropsychopharmacology*. 2023;48(3):529–39.
  26. Bredewold R, Washington C, Veenema AH. Vasopressin regulates social play behavior in sex-specific ways through glutamate modulation in the lateral septum. *Neuropsychopharmacology*. 2024;9:1–10.
  27. Wang D, Zhao D, Wang W, Hu F, Cui M, Liu J, Meng F, Liu C, Qiu C, Liu D, et al. How do lateral septum projections to the ventral CA1 influence sociability? *Neural Regeneration Res*. 2024;19(8):1789–801.
  28. Carus Cadavieco M, Gorbati M, Ye L, Bender F, van der Veldt S, Kosse C, Börgers C, Lee SY, Ramakrishnan C, Hu Y, et al. Gamma oscillations organize top-down signalling to hypothalamus and enable food seeking. *Nature*. 2017;542(7640):232–6.
  29. Okuda Y, Li D, Maruyama Y, Sonobe H, Mano T, Tainaka K, Shinohara R, Furiyashiki T. The activation of the piriform cortex to lateral septum pathway during chronic social defeat stress is crucial for the induction of behavioral disturbance in mice. *Neuropsychopharmacology*. 2024;12:1–13.
  30. Xiao Q, Zhou X, Wei P, Xie L, Han Y, Wang J, Cai A, Xu F, Tu J, Wang L. A new GABAergic somatostatin projection from the BNST onto accumbal parvalbumin neurons controls anxiety. *Mol Psychiatry*. 2021;26(9):4719–41.
  31. Lin S, Zhu MY, Tang MY, Wang M, Yu XD, Zhu Y, Xie SZ, Yang D, Chen J, Li X-M. Somatostatin-positive neurons in the rostral Zona incerta modulate innate fear-induced defensive response in mice. *Neurosci Bull*. 2023;39(2):245–60.
  32. Wang X, Zhang Y, Luo S, Zhao K, Gao C, Mei D, Duan Y, Hu S. Restoration of nNOS expression rescues autistic-like phenotypes through normalization of AMPA receptor-mediated neurotransmission. *Mol Neurobiol*. 2024;61(9):6599–612.
  33. Jang S, Park I, Choi M, Kim J, Yeo S, Huh SO, Choi JW, Moon C, Choe HK, Choe Y, et al. Impact of the circadian nuclear receptor REV-ERBs in dorsal Raphe 5-HT neurons on social interaction behavior, especially social preference. *Exp Mol Med*. 2023;55(8):1806–19.
  34. Wang F, Sun H, Chen M, Feng B, Lu Y, Lyu M, Cui D, Zhai Y, Zhang Y, Zhu Y, et al. The thalamic reticular nucleus orchestrates social memory. *Neuron*. 2024;112:1–18.
  35. Kalmbach A, Hedrick T, Waters J. Selective optogenetic stimulation of cholinergic axons in neocortex. *J Neurophysiol*. 2012;107(7):2008–19.
  36. Wang X, Mei D, Gou L, Zhao S, Gao C, Guo J, Luo S, Guo B, Yang Z, Wang Q, et al. Functional evaluation of a novel GRIN2B missense variant associated with epilepsy and intellectual disability. *Neuroscience*. 2023;526:107–20.
  37. Chen D, Lou Q, Song X-J, Kang F, Liu A, Zheng C, Li Y, Wang D, Qun S, Zhang Z, et al. Microglia govern the extinction of acute stress-induced anxiety-like behaviors in male mice. *Nat Commun*. 2024;15(1):449.
  38. Lee S, Jung WB, Moon H, Im GH, Noh YW, Shin W, Kim YG, Yi JH, Hong SJ, Jung Y, et al. Anterior cingulate cortex-related functional hyperconnectivity underlies sensory hypersensitivity in Grin2b-mutant mice. *Mol Psychiatry*. 2024;4(2):100289.
  39. Cho JY, Rumschlag JA, Tsvetkov E, Proper DS, Lang H, Berto S, Assali A, Cowan CW. MEF2C hypofunction in GABAergic cells alters sociability and prefrontal cortex inhibitory synaptic transmission in a sex-dependent manner. *Biol Psychiatry Global Open Sci*. 2024;4(2):100289.
  40. Hu H, Cavendish JZ, Agmon A. Not all that glitters is gold: off-target recombination in the somatostatin-IRES-Cre mouse line labels a subset of fast-spiking interneurons. *Front Neural Circuits*. 2013;7:195.
  41. Contractor A, Ethell IM, Cailliau CP. Cortical interneurons in autism. *Nat Neurosci*. 2021;24(12):1648–59.
  42. Wong JC, Grieco SF, Dutt K, Chen L, Thelin JT, Inglis GAS, Parvin S, Garraway SM, Xu X, Goldin AL, et al. Autistic-like behavior, spontaneous seizures, and increased neuronal excitability in a Scn8a mouse model. *Neuropsychopharmacology*. 2021;46(11):2011–20.
  43. Lyu TJ, Ma J, Zhang XY, Xie GG, Liu C, Du J, Xu YN, Yang DC, Cen C, Wang MY, et al. Deficiency of FRMD5 results in neurodevelopmental dysfunction and autistic-like behavior in mice. *Mol Psychiatry*. 2024;29(5):1253–64.
  44. Serikov A, Martsishevskaya I, Shin W, Kim J. Protocol for in vivo dual-color fiber photometry in the mouse thalamus. *STAR Protoc*. 2024;5(2):102931.
  45. Li J, Sun X, You Y, Li Q, Wei C, Zhao L, Sun M, Meng H, Zhang T, Yue W, et al. Auts2 deletion involves in DG hypoplasia and social recognition deficit: the developmental and neural circuit mechanisms. *Sci Adv*. 2022;8(9):1238.
  46. Chen D, Wang C, Li M, She X, Yuan Y, Chen H, Zhang W, Zhao C. Loss of Foxg1 Impairs the development of cortical SST-interneurons leading to abnormal emotional and social behaviors. *Cereb Cortex*. 2019;29(8):3666–82.
  47. Chen Z, Han Y, Ma Z, Wang X, Xu S, Tang Y, Vyssotski AL, Si B, Zhan Y. A prefrontal-thalamic circuit encodes social information for social recognition. *Nat Commun*. 2024;15(1):1036.
  48. Walsh JJ, Christoffel DJ, Heifets BD, Ben-Dor GA, Selimbeyoglu A, Hung LW, Deisseroth K, Malenka RC. 5-HT release in nucleus accumbens rescues social deficits in mouse autism model. *Nature*. 2018;560(7720):589–94.
  49. Sun Q, Li X, Li A, Zhang J, Ding Z, Gong H, Luo Q. Ventral hippocampal-prefrontal interaction affects social behavior via parvalbumin positive neurons in the medial prefrontal cortex. *iScience*. 2020;23(3):100894.

## Publisher's note

Springer Nature remains neutral with regard to jurisdictional claims in published maps and institutional affiliations.